CHARACTERIZATION OF SYNTHETIC Fe^{3+}-Fe^{2+}-Al-Mg SMECTITES. V. K. Fox[*1], R. J. Kupper[2], B.L. Ehlmann[1,3], J. G. Catalano[2], , R. D. Nickerson[2], S. M. Katz[2], A. A. White[2] [1]California Institute of Technology, Pasadena, CA 91125, USA; [2]Washington University in St Louis, Saint Louis, MO 63130, USA, [3]Jet Propulsion Laboratory, Pasadena, CA 91109, USA (vfox@caltech.edu)

Introduction: Secondary minerals produced by aqueous alteration of crustal rocks provide critical clues about the geochemistry, oxidation state, and extent of aqueous activity in the environment in which the secondary minerals formed. Therefore, alteration minerals can be key indicators of the geological history and habitability of objects throughout the solar system, provided that such minerals can be reliably detected and adequately characterized on other planetary bodies. Due to their ubiquity and geochemical sensitivity to their formation environment, Fe-, Mg-, and Al-bearing smectites are key target materials in planetary exploration. Despite their importance in planetary science and many studies detailing Martian clays [1–3], smectite clays have not been comprehensively characterized as standards to allow for accurate and nuanced remote sensing-based identification and quantification. Smectite composition can vary nearly continuously between Fe-, Mg-, and Al-rich end members by octahedral cation substitution, along with Al substitution for Si in the tetrahedral layer to balance charge [4,5]. The composition and iron oxidation state can be indicative of the conditions in which the clay minerals formed [6].

Here we present initial characterization efforts of 16 intermediate composition smectite clay samples, including both ferric and ferrous samples to further examine the role of oxidation state in smectite identification. Reflectance spectroscopy and Raman spectroscopy are complementary techniques, as both measure spectral features due to the molecular bond energies in mineral structures. Reflectance spectroscopy is the most frequently employed remote sensing method on Mars to identify mineralogy on the global scale, and Raman spectroscopy will be available to interrogate samples at the sub-millimeter scale on the Mars 2020 rover.

Methods: Smectites were synthesized using a sol-gel procedure with hydrothermal aging [7]. The compositions were determined by lithium metaborate digestion followed by analysis using inductively-coupled plasma optical emission spectroscopy. Each sample was confirmed to be a single phase smectite using X-ray diffraction on a Bruker D8 Advance diffractometer; ferrous samples were measured under an airtight acrylic dome to preserve anoxic conditions.

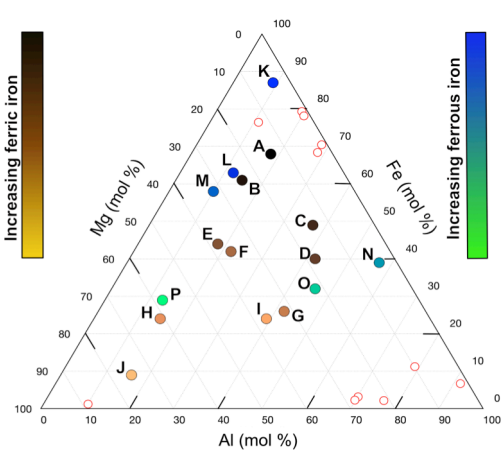The spectral reflectance was collected using an ASD field spectrometer (0.4-2.5 μm)

Figure 1. Ternary diagram showing the molar percentage of ferric/ferrous iron (brown-tan and blue-green, respectively), aluminum and magnesium of the 16 smectite samples. Open red circles indicate the compositions of common smectite spectral standards.

and a Nicolet FTIR spectrometer (1.5-~45 μm). VNIR spectra of the ferrous iron samples were obtained within an environmental chamber purged with Ar to minimize oxidation. Raman patterns were collected on loosely-packed powdered samples with a Renishaw M1000 micro Raman spectrometer using a 532 nm excitation wavelength between 100 and 4000 cm^{-1}.

Composition and Structure: The 16 samples were synthesized with compositions intermediate to widely used standards [8] (Figure 1). Six of the samples are ferrous smectites, which are uncommon in terrestrial studies but highly relevant to planetary science[6,7].

| Sample	Measured Formula	Octahedral Occupancy	Fe(II)/Fe(III)
A	$Ca_{0.36}Na_{0.09}[Fe^{III}_{1.69}Mg_{0.40}][Si_{3.32}Al_{0.51}Fe^{III}_{0.17}]O_{10}(OH)_2$	2.09	0.00
B	$Ca_{0.28}[Fe^{III}_{1.54}Mg_{0.64}][Si_{3.55}Al_{0.39}Fe^{III}_{0.06}]O_{10}(OH)_2$	2.18	0.00
C	$Ca_{0.34}Na_{0.20}[Fe^{III}_{1.24}Mg_{0.37}Al_{0.40}][Si_{3.44}Al_{0.56}]O_{10}(OH)_2$	2.01	0.00
D	$Ca_{0.35}Na_{0.21}[Fe^{III}_{1.04}Mg_{0.46}Al_{0.54}][Si_{3.45}Al_{0.55}]O_{10}(OH)_2$	2.04	0.00
E	$Ca_{0.40}[Fe^{III}_{1.06}Mg_{0.93}Al_{0.15}][Si_{3.70}Al_{0.30}]O_{10}(OH)_2$	2.14	0.00
F	$Ca_{0.32}Na_{0.03}[Fe^{III}_{0.98}Mg_{0.84}Al_{0.30}][Si_{3.80}Al_{0.20}]O_{10}(OH)_2$	2.12	0.00
G	$Ca_{0.23}[Fe^{III}_{0.69}Mg_{1.12}Al_{0.53}][Si_{3.66}Al_{0.34}]O_{10}(OH)_2$	2.13	0.00
H	$Ca_{0.39}[Fe^{III}_{0.68}Mg_{1.75}Al_{0.02}][Si_{3.60}Al_{0.40}]O_{10}(OH)_2$	2.34	0.00
I	$Ca_{0.30}Na_{0.26}[Fe^{III}_{0.57}Mg_{0.92}Al_{0.64}][Si_{3.67}Al_{0.33}]O_{10}(OH)_2$	2.45	0.00
J	$Ca_{0.37}[Fe^{III}_{0.27}Mg_{2.31}Al_{0.08}][Si_{3.60}Al_{0.40}]O_{10}(OH)_2$	2.66	0.00
K	$Ca_{0.23}[Fe_{2.51}Al_{0.26}Mg_{0.12}][Si_{3.51}Al_{0.49}]O_{10}(OH)_2$	2.89	89.00
L	$Ca_{0.31}[Fe_{1.70}Al_{0.33}Mg_{0.67}][Si_{3.63}Al_{0.37}]O_{10}(OH)_2$	2.70	86.00
M	$Ca_{0.29}Na_{0.05}[Fe_{1.61}Al_{0.29}Mg_{0.92}][Si_{3.46}Al_{0.54}]O_{10}(OH)_2$	2.82	93.10
N	$Ca_{0.27}Na_{0.08}[Fe_{0.89}Al_{1.29}Mg_{0.10}][Si_{3.54}Al_{0.46}]O_{10}(OH)_2$	2.28	90.00
O	$Ca_{0.28}Na_{0.12}[Fe_{0.75}Al_{1.08}Mg_{0.50}][Si_{3.56}Al_{0.44}]O_{10}(OH)_2$	2.33	85.40
P	$Ca_{0.29}Na_{0.06}[Fe_{0.80}Al_{0.35}Mg_{1.57}][Si_{3.57}Al_{0.43}]O_{10}(OH)_2$	2.72	86.60
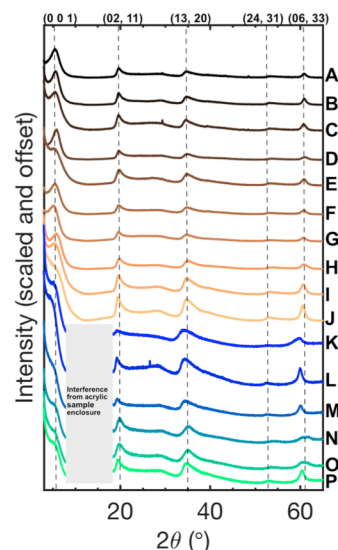
Figure 2. X-Ray Diffraction patterns of the 16 smectite samples. Shifts in the (06, 33) peak indicate structural changes from dioctahedral to more trioctahedral coordination.
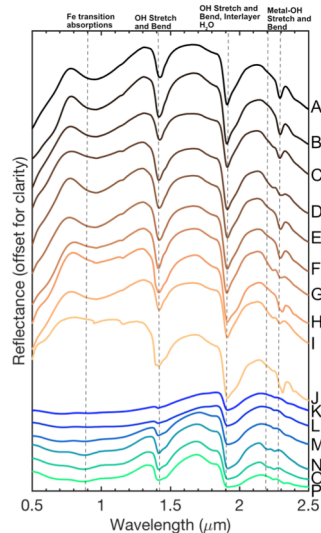

Figure 3. Spectral reflectance from 0.5-2.5 µm of the 16 samples. Deep features around 1.4 and 1.9µm are due to water within the interlayer, and are dependent on humidity.
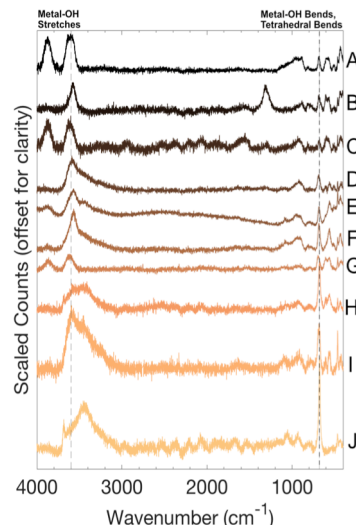

Figure 4. Raman spectra of the ferric smectite samples obtained using a 532 nm excitation laser. The 532 nm excitation wavelength is equivalent to the Raman spectrometry system planned for the SuperCam instrument designed for the Mars 2020 rover mission.

The octahedral occupancies as derived from the mineral formulas (Table 1) indicate that most of the ferric samples, with the exception of the most magnesium-rich samples (H,I,J), are dioctahedral in nature, whereas the magnesium rich or ferrous samples are mixed dioctahedral and trioctahedral in structure. The XRD measurements of the (06,33) band are consistent with this finding (Figure 2).

Reflectance Spectroscopy: Visible to near infrared (VNIR) reflectance spectroscopy is the most common method of identifying smectite clays on Mars, particularly from orbit. Ferrous smectites are particularly underrepresented in most spectral databases. Ferric versus ferrous iron in smectites particularly shapes the 0.5-1 µm spectral range (Figure 3); deep transition absorptions dominate when ferric iron comprises more than 15 mol%, whereas samples rich in ferrous iron have broader absorptions and a distinct overall spectral shape. The presence of ferrous iron also shifts the characteristic metal-OH combination absorptions between 2.1 and 2.5 µm to shorter wavelengths compared to the ferric-bearing samples. Overall the spectral contrast of the ferrous samples is less than that of the ferric smectites, though clumping of particles lowering albedo is something we are working on controlling as we remove more water from the ferrous smectite samples.

Raman Spectroscopy: Raman peaks between 3500 and 4000 cm^{-1} are sensitive to the metal-OH stretching modes; peaks shift to shorter Raman shifts as the iron content of the samples increase (Figure 4). The broad hump at 3400 cm^{-1} in most of the samples is due to water within the mineral structure. Peaks in the 150-800 cm^{-1} range are caused by the bending modes of both the octahedrally-coordinated cations and the tetrahedral silicon and aluminum. The peak around 680 cm^{-1} in particular is dependent on whether the smectite is dioctahedrally or trioctahedrally coordinated, such that the mixed coordination samples have a slightly shorter Raman shifts [9].

Future Work: Spectral measurements of these 16 smectite clay samples will be compiled into reference libraries to improve analysis of planetary data sets, particularly relevant to Martian remote sensing methods. Instrumentation is being adapted to allow mid-infrared reflectance and Raman spectral measurements of the ferrous iron-bearing samples which minimize the risk of oxidation during analysis.

References: [1] Michalski J. R. et al. (2015) *Earth and Planetary Science Letters* **427**, 215–225. [2] Bishop J. L. et al. (2008) *Science* **321**, 830–833. [3] Bristow T. F. et al. (2018) *Science Advances* **4**, eaar3330. [4] Grauby O. et al. (1994) *European Journal of Mineralogy* 99–112. [5] Andrieux P. and Petit S. (2010) *Applied Clay Science* **48**, 5–17. [6] Catalano J. G. (2013) *J. Geophys. Res. Planets* **118**, 2124–2136. [7] Chemtob S. M. et al. (2015) *J. Geophys. Res. Planets* **120**, 2014JE004763. [8] Gates W. P. (2005) in: Kloprogge, J.T. (Ed.), *CMS Workshop Lectures*. [9] Wang A. et al. (2015) *J. Raman Spectrosc.* **46**, 829–845.